

pH-Induced Change in the Rate-Determining Step for the Hydrolysis of the Asp/Asn-Derived Cyclic-Imide Intermediate in Protein Degradation

Minli Xie, David Vander Velde, Martha Morton, Ronald T. Borchardt, and Richard L. Schowen*

Department of Pharmaceutical Chemistry and
NMR Laboratory, The University of Kansas
Lawrence, Kansas 66046

Received February 26, 1996

The ring-opening reaction of the cyclic imide shown in Scheme 1, the key intermediate in the degradation of proteins and peptides at Asp and Asn "hot spots,"¹ proceeds by rate-limiting C–N bond fission at pH 1–4 and by rate-limiting attack of water at higher pHs, as shown by ¹⁸O-exchange into both carbonyl groups of the cyclic imide below pH 4 but not at higher pHs (Figure 1). The transition states for formation and decomposition of the intermediate T_{β}° are identical to those for cyclic-imide formation at Asp residues in proteins. Thus protein instability at pH > 5, deriving from cyclization at Asp residues to form the cyclic imide, results from a relatively low free energy of the transition state for the expulsion of water from the tetrahedral intermediate T_{β}° (Scheme 1), following rapid, reversible C–N bond formation. The greater stability of proteins at pH < 5 results from a relatively high free energy of the transition state for C–N bond formation to generate T_{β}° . Similar considerations may apply to cyclization at Asn residues in proteins.

Figure 1 shows the pH-rate profile for the ¹⁸O-exchange and hydrolysis reactions of the two cyclic imides shown in Scheme 1. In the region of pH 6–8, the filled triangles denote the rates of loss of the cyclic imide at 50 °C determined by capillary electrophoresis (CE). For pH 5.9–8.0, no ¹⁸O-exchange into the carbonyl groups of the cyclic imide was observed ($k < 1.6 \times 10^{-8} \text{ s}^{-1}$), which indicates that the attack of water on both the α - and β -carbonyl groups is rate determining. However, in the region of pH 1–4, exchange was observed: the filled symbols denote the rate constants for ¹⁸O-exchange into the α -carbonyl group (squares) and the β -carbonyl group (circles) of the cyclic imide, while only minimal hydrolysis was observed at pH 3.9 (k ca. $8 \times 10^{-8} \text{ s}^{-1}$), and none at pH 1.9 ($k < 3 \times 10^{-10} \text{ s}^{-1}$). The results indicate that in the pH region of 1.9–4, the rate-determining step of cyclic-imide breakdown is C–N bond fission (leaving-group expulsion), while in the pH range 5.5–8, the rate-determining step is C–O bond formation (water attack). A pH-induced change in the rate-determining step occurs at pH 4–5.5.

During studies of hydrolysis of the cyclic imide, CE provided a rapid, precise alternative to HPLC.³ The ¹³C–NMR method of Van Etten and co-workers⁴ was employed for the ¹⁸O-exchange studies. With a Bruker AM-500 NMR spectrometer operating at 125.77 MHz for ¹³C, the two carbonyl groups are well resolved with the α -carbonyl signal at 180.7 ppm and the β -carbonyl signal at 179.9 ppm in H₂¹⁸O (60–80%) solution with 20% D₂O. The signal for an ¹⁸O-labeled carbonyl has an upfield shift of 0.04 ppm from the original ¹⁶O-carbonyl signal,

(1) (a) Ahren, T. J.; Manning, M. C., Eds. *Stability of Protein Pharmaceuticals: Part A. Chemical and Physical Pathways of Protein Degradation*; Plenum Press: New York, 1992. (b) Aswad, D. W., Ed. *Deamidation and Isoaspartate Formation in Peptides and Proteins*; CRC Press, Boca Raton, FL, 1995.

(2) Capasso, S.; Kirby, A. J.; Salvadori, S.; Sica, F.; Zagari, A. *J. Chem. Soc., Perkin Trans. 2* **1995**, 437–442.

(3) (a) Nielsen, R. G.; Riggan, R. M.; Rickard, E. C. *J. Chromatogr.* **1989**, *480*, 393–401. (b) Wu, S.; Teshima, G.; Cacia, J.; Hancock, W. S. *J. Chromatogr.* **1990**, *516*, 115–122.

(4) Cortes, S. J.; Mega, T. L.; Van Etten, R. L. *J. Org. Chem.* **1991**, *56*, 943–947 and references cited therein.

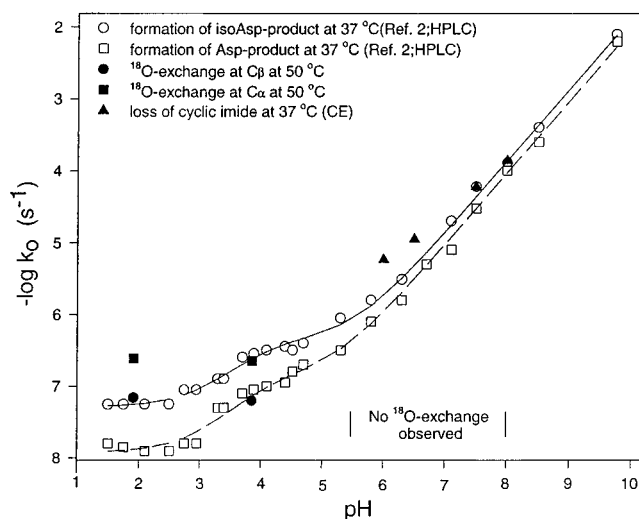
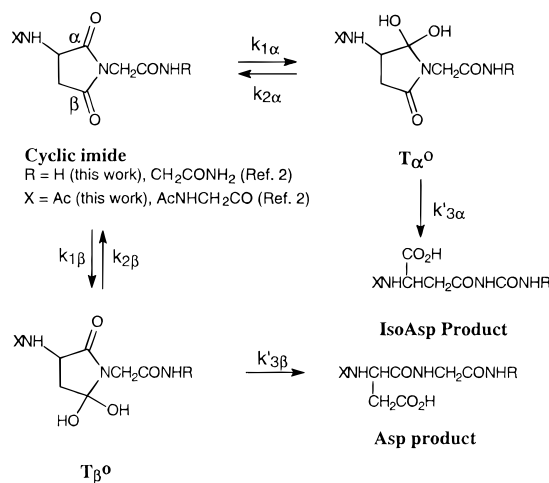


Figure 1. Rate constants of hydrolysis and ¹⁸O-exchange for the cyclic imides of Scheme 1 as a function of pH. Open symbols are from the work of Capasso *et al.*² at 37 °C. Filled symbols are from this work at 37 °C (hydrolysis) and 50 °C (exchange). The solid lines are plots of eq 1 with $10^7 k_{1W} = 4.85$ (α), 1.66 (β) s^{-1} ; $k_{1B} = 140$ (α), 100 (β) $\text{M}^{-1} \text{s}^{-1}$; $10^8 k_{3W} = 5.86$ (α), 1.30 (β) s^{-1} ; $k_{3B} = 5537$ (α), 1544 (β) $\text{M}^{-1} \text{s}^{-1}$, which are in acceptable agreement with values calculated by Capasso *et al.*² on the basis of a rate law omitting k_{3W} . The rate constants shown for isotope exchange are, in terms of those in Scheme 1, given by $k_{1x} k_{2x}/2(k_{2x} + k'_{3x})$, where $x = \text{either } \alpha \text{ or } \beta$.

Scheme 1



permitting the concentration of ¹⁸O-labeled cyclic imides to be followed as a function of time (Figure 2). The relative amount of ¹⁶O- and ¹⁸O-carbonyl groups can be determined from the peak heights assuming that there is no isotope effect on the NOEs⁴ of the carbonyl carbon signals.

These findings are wholly consistent with the mechanism proposed by Capasso *et al.*² on the basis of extensive kinetic studies, a part of which are shown in Figure 1. The ¹⁸O-exchange results now reported in this work show unambiguously that leaving-group expulsion is rate limiting below pH 4 and water attack rate limiting above pH 5.5. The kinetic results alone could not specify which step is rate limiting in the various pH ranges. The solid lines in Figure 1 are plots of eq 1, the kinetic law for the proposed model² extended to include an uncatalyzed route of C–N bond fission at very low pH. Hydrolysis is represented in Scheme 1 as proceeding by attack of water at each of the carbonyl groups to form tetrahedral intermediates (shown in the neutral forms T_{α}° and T_{β}°) with total rate constants $k_{1\alpha}$ and $k_{1\beta}$, followed by breakdown of the

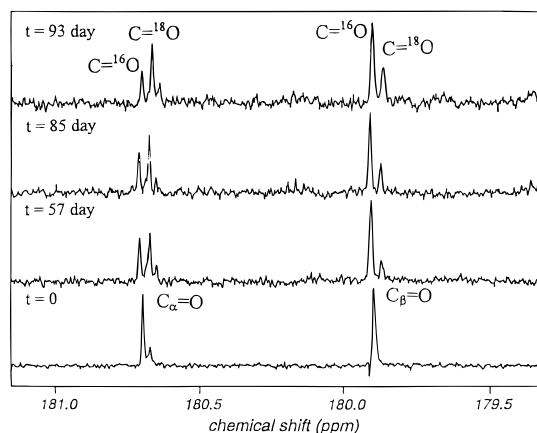


Figure 2. ^{13}C -NMR spectra of the cyclic imide (Scheme 1) showing ^{18}O -exchange as a function of time. Reactions were carried out using 173 mM cyclic imide in 0.1 M phosphate buffer (pH 3.9) at 50 °C.

tetrahedral intermediates by C–N bond fission (total rate constants $k'_{3\alpha}$ and $k'_{3\beta}$) to give the Asp product (from $\text{T}_{\alpha}^{\circ}$) and isoAsp product (from T_{β}°). The pH-rate profiles of Capasso *et al.*² and the ^{18}O -exchange data reported here are consistent with contributions to both formation and breakdown of $\text{T}_{\alpha}^{\circ}$ and T_{β}° of an uncatalyzed pathway ($k_{1\text{W}}$, $k'_{3\text{W}}$) and a hydroxide-catalyzed pathway ($k_{1\text{B}}$, $k'_{3\text{B}}$). This mechanism gives the kinetic law of eq 1 where $k_{3\text{B}} = (k_{1\text{B}}k'_{3\text{B}}/k_{2\text{B}})$ and $k_{3\text{W}} = (k_{1\text{W}}k'_{3\text{W}}/k_{2\text{W}})$.

$$k_0 = \frac{(k_{1\text{B}}[\text{OH}^-] + k_{1\text{W}})(k_{3\text{B}}[\text{OH}^-] + k_{3\text{W}})}{k_{1\text{B}}[\text{OH}^-] + k_{1\text{W}} + k_{3\text{B}}[\text{OH}^-] + k_{3\text{W}}} \quad (1)$$

Asn and Asp are hot spots in the nonenzymic degradation of proteins and peptides, leading to the formation of isoAsp and Asp sites, resulting in possibly altered properties that can affect the biological activities of the proteins and peptides.^{5,6} In addition to deamidation of Asn residues with conversion to Asp and isoAsp sites, and conversion of Asp residues to isoAsp residues, racemization is accelerated in the cyclic imide, leading to introduction of D-Asp and D-isoAsp. These reactions are components of the *in vivo* degradation of proteins connected with the aging process and with certain pathological states. For example, the aggregation of degraded isoAsp-containing β -amyloid peptides has been found in Alzheimer's-disease-affected brains.⁷ An enzyme, D-aspartyl/L-isoaspartyl protein methyltransferase, which repairs D-Asp and L-isoAsp residues in degraded proteins, is found in all cells and tissues examined to

date.⁸ *In vitro* studies have also indicated that Asn/Asp degradation is one of the factors contributing to the irreversible thermal inactivation of proteins,⁹ and is a major source of instability of protein and peptide pharmaceuticals during preparation and storage.¹

Extensive studies have shown that cyclic imides of the type shown in Scheme 1 are the critical intermediates in both *in vivo* and *in vitro* protein degradation. Cyclic imides are formed by nucleophilic attack of the backbone nitrogen of the $i + 1$ residue on the side-chain carbonyl of the i residue, with subsequent expulsion of ammonia (Asn) or water (Asp). The transition states for these processes may be important in developing biotechnologies. Catalytic antibodies prepared against haptens resembling the intermediates $\text{T}_{\alpha}^{\circ}$ and T_{β}° , and thus (by Hammond's postulate) the cyclization/hydrolysis transition states have been found to catalyze both cyclic-imide formation and hydrolysis in peptides. Such antibodies could lead to the design of pharmaceutical agents for degrading undesired peptides and proteins.¹⁰ The present studies bear on both hydrolysis of the cyclic intermediate (which determines the ratio of Asp and isoAsp products in the degraded polypeptide) and formation of the intermediate (since the transition states for hydrolysis at $\text{C}\beta$ should be the same as those for ring closure at Asp centers and are similar to those for ring closure at Asn centers). The data presented in Figure 1 indicate that for both Asp and isoAsp formation, the rate-limiting process at pH 1–3 is uncatalyzed ring opening (rate constant $k_{3\text{W}}$ in eq 1). At pH 3–4, base-catalyzed ring opening ($k_{3\text{B}}$) becomes significant. At around pH 4–5, the rate-determining step shifts to uncatalyzed attack of water on the cyclic imide ($k_{1\text{W}}$). Above pH 6, base-catalyzed attack of water at carbonyl ($k_{1\text{B}}$) dominates. The values of the rate constants (caption of Figure 1) confirm the observation that the isoAsp product, which is always in 2–4 fold excess, dominates to a smaller degree as the pH rises. Thus the product-expulsion transition state (rate limiting at low pH) favors $\text{C}\alpha$ –N fission over $\text{C}\beta$ –N fission somewhat more than the water-attack transition state (rate limiting at high pH) favors attack at $\text{C}\alpha$ over attack at $\text{C}\beta$. It is still not possible to specify the detailed origin of preferred water attack and preferred leaving-group expulsion at $\text{C}\alpha$, which presumably result from combined electronic, steric and possibly intramolecular catalytic effects. This point remains unclear and is under investigation.

Acknowledgment. We thank the Pharmaceutical Research and Manufacturers of America Foundation for a Fellowship in Advanced Predoctoral Training in Pharmaceutics for M.X.

Supporting Information Available: Experimental details for ^{18}O -exchange experiments, electropherogram and NMR spectra, and table of kinetic results (11 pages). See any current masthead page for ordering and Internet access instructions.

JA9606182

(8) Clarke, S. *Annu. Rev. Biochem.* **1985**, *54*, 479–506.

(9) Ahren, T. J.; Klibanov, A. M. *Prot. Struct., Folding, Des.* **1986**, 283–289.

(10) (a) Gibbs, R. A.; Taylor, S.; Benkovic, S. J. *Science* **1992**, *258*, 803–805. (b) Liotta, L. J.; Benkovic, P. A.; Miller, G. P.; Benkovic, P. A. *J. Am. Chem. Soc.* **1993**, *115*, 350–351. (c) Liotta, L. J.; Gibbs, R. A.; Taylor, S. D.; Benkovic, P. A.; Benkovic, S. J. *J. Am. Chem. Soc.* **1995**, *117*, 4729–4741.

(5) Cleland, J. L.; Powell, M. F.; Shire, S. L. *Crit. Rev. Ther. Drug Carrier Syst.* **1993**, *10*, 307–377.

(6) Clarke, S.; Stephenson, R. C.; Lowenson, J. D. In *Stability of Protein Pharmaceuticals, Part A: Chemical and Physical Pathways of Protein Degradation*; Ahren, T. J., Manning, M. C., Eds.; Plenum Press: New York, **1992**; pp 1–29.

(7) (a) Roher, A. E.; Lowenson, J. D.; Clarke, S.; Wolkow, C.; Wang, R.; Cotter, R. J.; Reardon, I. M.; Zürcher-Neely, H. A.; Heinrikson, R. L.; Ball, M. J.; Greenberg, B. D. *J. Biol. Chem.* **1993**, *268*, 3072–3083. (b) Fabian, H.; Szendrei, G. I.; Mantsch, H. H.; Greenberg, B. D.; Ötvös, L., Jr. *Eur. J. Biochem.* **1994**, *221*, 959–964.